Coherent spin dynamics of excitons in strained monolayer semiconductors

M. M. Glazov
Ioffe Institute, 194021 Saint Petersburg, Russia

(Received 13 October 2022; revised 16 November 2022; accepted 16 November 2022; published 20 December 2022)

We develop a model of the coherent exciton spin-valley dynamics in two-dimensional transition-metal dichalcogenides under elastic strain. The strain splits the exciton radiative doublet into linearly polarized states. Consequently, it induces an effective magnetic field acting on the exciton pseudospin, and it causes its precession. As a result, under circularly polarized excitation, the circular polarization of excitons oscillates with time, and a time-oscillating linear polarization appears. We study the competition of the strain-induced effective magnetic field with the field caused by the exciton longitudinal-transverse splitting. We uncover different regimes of coherent spin dynamics of two-dimensional excitons. In particular, we show that for sufficiently large strain-induced and longitudinal-transverse splittings, two frequencies related to these splittings appear in the exciton circular polarization beats.

DOI: 10.1103/PhysRevB.106.235313

I. INTRODUCTION

More than 60 years ago, Rashba predicted the so-called resonant (also termed annihilation) interaction between an electron and a hole in Wannier-Mott excitons [1]. That work helped to resolve contradictions between previous works on the exciton fine structure within the effective-mass approximation [2] and the general theory of polaritons in semiconductors [3–5]. Reference [1] demonstrated the existence of the long-range exchange interaction between an electron and a hole in semiconductors, and it laid the foundation for a consistent theory of exchange interaction in excitons and their energy spectrum fine structure developed in later works [6–8].

Nowadays, the electron-hole exchange interaction is actively studied in the context of semiconductor quantum wells [9–11], quantum dots and nanocrystals [12–19], and two-dimensional (2D) semiconductors [20–26]. The growing family of 2D semiconductors includes transition-metal dichalcogenide monolayers (TMDC MLs), which are renowned for their outstanding optical, excitonic, and electronic properties, and the remarkable spin-valley physics; these materials can serve as a basis for van der Waals heterostructures, providing additional degrees of control of spin and valley degrees of freedom [27–30].

Electronic properties of 2D materials can be manipulated by elastic strains [31,32], which can also be applied locally [33], making it possible to confine [34,35] and steer excitons [36–41], see also Ref. [42] and references therein for review. Much less is known about the strain effect on the exciton fine structure: The splitting of the exciton radiative doublet formed of otherwise degenerate states emitting in σ^+ and σ^- circular polarizations into linearly polarized states has been reported in Refs. [43,44], but a detailed systematic study of the effect has been missing until recently. In our work [45], we have derived the effective Hamiltonian of the exciton radiative doublet in the presence of elastic strain, and we demonstrated both experimentally and theoretically the consequences of strain on the exciton fine-structure properties: The strain modifies optical selection rules and induces, via the electron-hole exchange interaction, a fine-structure splitting of the exciton radiative doublet. Interestingly, in 2D TMDCs the strain also results in spin-dependent wave-vector linear terms in the effective Hamiltonians of electrons, holes, and excitons [45], similar to Rashba spin-orbit terms in conventional semiconductors and semiconductor nanosystems [46–49].

The strain-induced splitting of the exciton radiative doublet should also result in coherent quantum beats of the excitons if a superposition of linearly polarized eigenstates is excited by a circularly polarized light. This effect is analogous to the electron spin precession in the external magnetic field [14]. The studies of coherent spin dynamics via time- and polarization-resolved photoluminescence and time-resolved pump-probe experiments provide deep insight into the fine structure, allow one to uncover splittings hidden by an inhomogeneous broadening of optical resonances, and provide access to the kinetic processes governing relaxation between the split levels [50,51]. While calculations of the exciton energy splitting in the presence of strain and induced linear polarization are sufficient to interpret optical spectroscopy experiments such as absorption/reflection or photoluminescence, the model of coherent spin dynamics of excitons in 2D TMDCs is needed to form a basis for future time-resolved experimental studies of exciton spin dynamics in strained monolayers. Such a theory is presented in this work. Furthermore, the exciton fine-structure splitting is contributed both by the exciton wave-vector-independent strain-induced contribution and a wave-vector-dependent exciton longitudinal-transverse splitting [20–22]. An interplay of these two contributions, as we show here, results in specific features of the exciton quantum spin beats, and for sufficiently large splittings it allows one to disentangle these contributions in the spin dynamics.

Here we study theoretically manifestations of the exciton fine structure in TMDC MLs, particularly the strain-induced

contributions, in the coherent spin dynamics of excitons. We analyze exciton spin beats in the presence of strain, and we address the interplay of exciton longitudinal-transverse splitting and strain in exciton spin precession and damping. We briefly discuss the role of energy relaxation processes and inhomogeneities of the strain.

II. MODEL

We recall that in 2D TMDCs, bright excitons arise from optical transitions in two valleys $\boldsymbol{K}_+$ and $\boldsymbol{K}_-$ that are active in σ^+ and σ^- circular polarizations, and superpositions of these states are active in linear polarizations [24,52–59]. These two states can be mapped to the spin 1/2 states. Thus the exciton radiative doublet can be described in terms of pseudospin [14].

An effective Hamiltonian describing the fine structure of a radiative doublet of a two-dimensional exciton in the presence of strain can be recast in the form

$$\mathcal{H} = \frac{\hbar}{2}(\hat{\boldsymbol{\sigma}} \cdot \boldsymbol{\Omega}_{\boldsymbol{K}}), \tag{1}$$

where $\hat{\boldsymbol{\sigma}} = (\hat{\sigma}_x, \hat{\sigma}_y, \hat{\sigma}_z)$ are the pseudospin Pauli matrices describing the exciton pseudospin: $\hat{\sigma}_z$ describes the circularly polarized states, $\hat{\sigma}_x$ and $\hat{\sigma}_y$ describe the linearly polarized components in the coordinate frames rotated by 45° with respect to each other [14,20], $\boldsymbol{K} = (K_x, K_y)$ is the two-dimensional translational motion wave vector of the exciton (the ML is in the xy plane), and $\boldsymbol{\Omega}_{\boldsymbol{K}}$ is the effective magnetic field acting on the exciton pseudospin [45],

$$\Omega_{x,\boldsymbol{K}} = \mathcal{A}(K)\left(K_x^2 - K_y^2\right) + \mathcal{B}(u_{xx} - u_{yy}), \tag{2a}$$

$$\Omega_{y,\boldsymbol{K}} = 2\mathcal{A}(K)K_xK_y + 2\mathcal{B}u_{xy}, \tag{2b}$$

$$\Omega_{z,\boldsymbol{K}} = \mathcal{C}[(u_{xx} - u_{yy})K_x - 2u_{xy}K_y]. \tag{2c}$$

Here u_{ij} $(i, j = x, y, z)$ are the Cartesian components of the strain tensor [60], and $\mathcal{A}(K)$, $\mathcal{B}$, and $\mathcal{C}$ are the parameters describing the exciton fine structure. The parameters $\mathcal{B}$ and $\mathcal{C}$ result from the strain. The product $\mathcal{A}(K)K^2$ is responsible for the longitudinal-transverse (LT) splitting of the excitonic states [20–22,25,61], $\mathcal{A} \neq 0$ in the absence of strain, and we disregard possible strain-induced modification of the function $\mathcal{A}$. Microscopically, the main contribution to the LT splitting of the two-dimensional excitons is provided by the long-range exchange interaction between the electron and hole, which can be treated as a process of (virtual) recombination and generation process of the electron-hole pair [1,6–8,11,13,20,25,45]. Accordingly, for a suspended monolayer,

$$\mathcal{A}(K) \approx \frac{\Gamma_0}{qK}, \tag{3}$$

with Γ_0 being the exciton radiative decay rate and $q = \omega_0/c$ being the light wave vector at the frequency of the exciton transition ω_0. For encapsulated monolayers, the long-range exchange interaction is partially screened, and $\mathcal{A}(K)$ becomes reduced as compared to Eq. (3), while the wave-vector dependence is approximately preserved [25]. Note that for the states within the light cone, $K < q$, Eq. (3) is inapplicable, $\mathcal{A}(K)$ is imaginary, and the exchange interaction results in the renormalization of the exciton radiative decay rates; such states are not considered here.

The parameters $\mathcal{B}$ and $\mathcal{C}$ describe the effects of anisotropic strain on the exciton fine structure. In particular, $\mathcal{B}$ is responsible for the splitting of excitonic states into linearly polarized components along the main axes of the strain tensor u_{ij}. The parameter $\mathcal{C}$ describes an effective magnetic field arising due to the exciton propagation in the presence of strain that appears for the excitons with finite center-of-mass momentum.

The mixed strain components u_{xz}, u_{yz}, if present, can couple dark excitonic states with bright ones. Here we disregard these effects for the following reasons: (i) In experimental settings such as those in Refs. [43–45], these mixed strain components are expected to be small compared to the in-plane ones; and (ii) due to an interplay of the exchange and spin-orbit interaction, typical energy splittings between bright and dark states are significant and exceed by far the strain-induced splittings. Here a possible exception could be $MoSe_2$ MLs with relatively small dark-bright splitting [62], which require a separate study.

Detailed analysis of the eigenstates of the Hamiltonian (1) and microscopic mechanisms behind the parameters $\mathcal{B}$ and $\mathcal{C}$ is presented in Ref. [45]. Here we focus on the exciton pseudospin dynamics in the presence of strain and interplay of the longitudinal-transverse and strain-induced contributions in the spin beats.

The dynamics of the radiative doublet is conveniently described in the density matrix approach [14,24,63,64] $\varrho_{\boldsymbol{K}} = n_{\boldsymbol{K}} + (\boldsymbol{s}_{\boldsymbol{K}} \cdot \boldsymbol{\sigma})$. Here $n_{\boldsymbol{K}}$ is the average occupancy of the state with the wave vector $\boldsymbol{K}$, and $\boldsymbol{s}_{\boldsymbol{K}}$ is the average value of the pseudospin in this state. Generally, $n_{\boldsymbol{K}}$ and $\boldsymbol{s}_{\boldsymbol{K}}$ obey a set of coupled kinetic equations,

$$\frac{\partial n_{\boldsymbol{K}}}{\partial t} = Q\{n, \boldsymbol{s}\}, \tag{4a}$$

$$\frac{\partial \boldsymbol{s}_{\boldsymbol{K}}}{\partial t} + \boldsymbol{s}_{\boldsymbol{K}} \times \boldsymbol{\Omega}_{\boldsymbol{K}} = \boldsymbol{Q}\{\boldsymbol{s}, n\}, \tag{4b}$$

where $Q\{n, \boldsymbol{s}\}$ and $\boldsymbol{Q}\{\boldsymbol{s}, n\}$ are the collision integrals for the exciton and pseudospin distribution functions, respectively. It follows from Eqs. (2) and (4) that the strain for excitonic pseudospin plays the role of an effective magnetic field applied in the plane of the structure, thus coherent spin beats are expected like those arising for electron spins in the presence of a real magnetic field [50].

III. RESULTS AND DISCUSSION

A. Analysis of parameters

Before proceeding to the numerical and analytical results, let us briefly estimate the parameters is question. The exciton LT splitting Ω_K^{LT} scales approximately linearly with the exciton wave vector; see Eqs. (2) and (3). Correspondingly, we present

$$\Omega_K^{\mathrm{LT}} = \mathcal{A}(K)K^2 = V_{\mathrm{LT}}K. \tag{5}$$

The parameter V_{LT} can be associated with the effective velocity arising due to the K-linear LT splitting. For suspended monolayer $V_{\mathrm{LT}} = \Gamma_0/q$, see Eq. (3). Depending on the system parameters, $V_{\mathrm{LT}} = 10^6, \ldots, 10^7$ cm/s.

Another parameter that has a dimension of velocity is the coefficient $\mathcal{C}$ at the strain-induced $\boldsymbol{K}$-linear Zeeman effect, Eq. (2c). According to Ref. [45], the parameter $\mathcal{C} \sim \gamma_3/\hbar$,

where γ_3 is related to the interband momentum matrix element in the $\boldsymbol{k}\cdot\boldsymbol{p}$ model. For $\gamma_3 \approx 3$ eV Å [65,66] we have $\mathcal{C} \approx 10^7$ cm/s. Since $\Omega_{z,\boldsymbol{K}}$ in Eq. (2) is determined by the product of $\mathcal{C}$ and strain components, the effective strain-induced velocity can be introduced as $V_{\text{strain}} = \mathcal{C}(u_{xx} - u_{yy})$. For reasonable strain values that do not exceed several percent, $V_{\text{strain}} \ll V_{\text{LT}}$. Thus, in most cases, the effect of the strain-induced $\boldsymbol{K}$-linear terms are negligible for excitons as compared to the LT splitting.

Next, let us compare the LT and strain-induced wave-vector-independent splittings. The former depends on the exciton center of momentum K that, in turn, depends on the excitation conditions and temperature. It can vary, in typical conditions, from fractions of meV to tens of meV in atomically thin crystals for reasonable $K \sim 10^6$ cm^{-1}. From analytical estimates and experimental data reported in Ref. [45] for reasonable values of uniaxial strain, the induced splitting $\hbar\mathcal{B}(u_{xx} - u_{yy}) \sim 1$ meV. Thus, typically, LT and strain-induced splittings can be comparable in magnitude. It is noteworthy that while particular parameters vary between different TMDC MLs, their orders of magnitude are similar due to the similarity of the crystalline and band structure. That is why we use generic values of parameters to illustrate the basic effects in coherent spin dynamics of excitons.

The dynamics of pseudospin is controlled not only by the magnitude of $\boldsymbol{\Omega}_{\boldsymbol{K}}$ in Eqs. (2) and (4b), but also by two more parameters that determine the kinetics of excitons: their mean kinetic energy $\bar{E}$ and scattering rate τ^{-1}. Typically, three parameters that have dimension of energy—$\hbar\Omega$ (with Ω being the characteristic value of $|\boldsymbol{\Omega}_{\boldsymbol{K}}|$), $\bar{E}$, and $\hbar/\tau$—can be comparable in magnitude for excitons in 2D TMDCs. This makes kinetic processes quite involved in such systems; see, e.g., Refs. [67–70]. Here we focus on the simplified description of the exciton pseudospin dynamics and assume that the applicability condition of the kinetic equations (4), $\bar{E} \gg \hbar/\tau$, is fulfilled. Also, for simplicity, we consider $\hbar\Omega \ll \bar{E}$, while the product $\Omega\tau$ can be arbitrary. Depending on whether the product $\Omega\tau$ is smaller or larger than unity, the pseudospin dynamics can be quite different. We stress that we are interested in the situations in which excitons are excited resonantly or quasiresonantly and the temperature is not too high. In this case, $\bar{E} \ll E_g$, where E_g is the band gap, and it is sufficient to use the approximation of parabolic isotropic dispersion for excitons and keep the lowest contributions in the wave vector $\boldsymbol{K}$ to the precession frequency $\boldsymbol{\Omega}_{\boldsymbol{K}}$; see Eq. (2).

B. Coherent spin dynamics of excitons

In what follows, we focus on the exciton pseudospin dynamics and take the collision integral in the form

$$\boldsymbol{Q}\{\boldsymbol{s}, n\} = -\frac{\boldsymbol{s}_{\boldsymbol{K}} - \bar{\boldsymbol{s}}_{\boldsymbol{K}}}{\tau}, \tag{6}$$

where τ is the scattering time and $\bar{\boldsymbol{s}}_{\boldsymbol{K}}$ is the angular-averaged pseudospin. The exciton lifetime and exciton energy relaxation are assumed to exceed by far τ and Ω^{-1}, which typically occurs for exciton scattering by acoustic phonons [69,71]. We also select the coordinate system where $u_{xy} = 0$, i.e., the x and y axes are the main axes of the strain, and we introduce the notation $u \equiv u_{xx} - u_{yy}$.

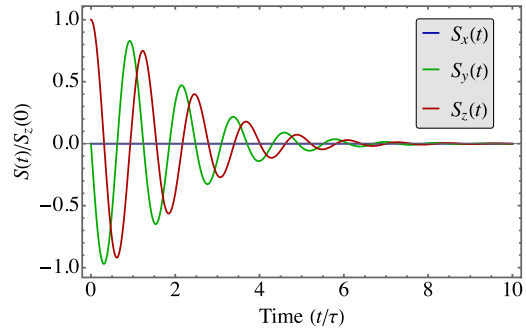

FIG. 1. Temporal dynamics of exciton pseudospin components $S_\alpha = \sum_{\boldsymbol{K}} s_{\alpha,\boldsymbol{K}}$ ($\alpha = x, y, z$) after pulsed circularly polarized excitation calculated by numerically solving kinetic Eq. (4). Calculation parameters are $\Omega_K^{\text{LT}}\tau = 1$, $\mathcal{B}u\tau = 5$, and $\mathcal{C} = 0$.

Figure 1 shows the exciton pseudospin dynamics for the uniaxial strain calculated numerically in the case of the resonant circularly polarized excitation by a short pulse: We solve the kinetic equation (4) numerically by decomposing the $\boldsymbol{s}_{\boldsymbol{K}}$ in the series of angular harmonics with the initial condition $s_{x,\boldsymbol{K}} = s_{y,\boldsymbol{K}} \equiv 0$, $s_{z,\boldsymbol{K}} \propto \delta(E_K - E_0)$ (cf. Ref. [72]). Here E_K is the exciton dispersion, E_0 is the excitation energy, and inelastic processes are neglected, thus the energy dependence of the pseudospin distribution function is preserved. The main features of the exciton pseudospin dynamics in strained monolayers are clearly seen from Fig. 1: Pronounced beats are present in the circular polarization S_z, and the conversion between the circular and linear polarization in the diagonal axes, S_y, is observed similarly to the polarization conversion in conventional semiconductor nanosystems [63,73–75]. Linear polarization in the (xy) axes, S_x, does not appear in this model, but it may arise due to redistribution of the excitons between the fine-structure split levels in the presence of inelastic processes and because of the strain-induced modification of the optical selection rules [45]; see also Ref. [76]. The band mixing at high exciton momenta (away from the $\boldsymbol{K}_\pm$ points of the Brillouin zone for electrons and holes) also results in a reduction of the degree of exciton optical orientation; see, e.g., Ref. [59]. These factors can be taken into account in our model by adjustment of initial conditions. Our model can also be applied to anisotropic 2D semiconductors where two close-in-energy excitonic states active in orthogonal linear polarization are present.

In Fig. 2, the evolution of the exciton circular polarization dynamics as a function of elastic strain is shown. At $\mathcal{B}u \to 0$, the effect of strain on the polarization beats is negligible and the dynamics is solely controlled by the long-range exchange interaction. In this case, it can be described by the following analytical formula (see Ref. [25] and references therein):

$$\frac{s_{z,K}(t)}{s_{z,K}(0)} = e^{-t/2\tau}\left(\cosh\frac{wt}{2\tau} + w^{-1}\sinh\frac{wt}{2\tau}\right), \tag{7}$$

where $w = \sqrt{(\Omega_K^{\text{LT}}\tau)^2 - 1/4}$. In particular, for $\Omega_K^{\text{LT}}\tau \gg 1$ the beats due to the exciton LT splitting are observed, and their damping is determined by the scattering time (the decay rate is 2τ). This is because a single scattering of exciton results in significant variation of $\boldsymbol{\Omega}_{\boldsymbol{K}}$ due to the change of the exciton

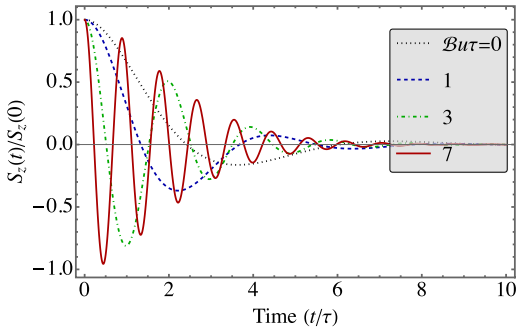

FIG. 2. Temporal dynamics of the z component of exciton pseudospin after pulsed circularly polarized excitation calculated by numerically solving kinetic Eq. (4) for different values of elastic strain (shown in the legend). Other parameters are the same as in Fig. 1.

wave vector, thus on the timescale $\sim\tau$ the coherence in spin dynamics breaks. At $\mathcal{B}u \gg \Omega_K^{\rm LT}$, the beats occur at the strain-related frequency, $\mathcal{B}u$. In the intermediate regime the situation is more involved; see below.

The role of the LT splitting in the strain-induced exciton pseudospin dynamics is illustrated in Fig. 3. Panel (a) shows the results for the circular polarization beats in the collision-dominated regime, $\Omega_K^{\rm LT}\tau = 0.3$. In this case, the exciton spin dynamics is described by analytical expressions similar to those for electron spin beats in magnetic field at anisotropic spin relaxation [77,78]:

$$\frac{s_{z,K}(t)}{s_{z,K}(0)} = \left[\cos\bar{\Omega}t - \frac{\Gamma_{zz}-\Gamma_{yy}}{2\bar{\Omega}}\sin\bar{\Omega}t\right]e^{-\bar{\Gamma}t}, \tag{8}$$

where

$$\bar{\Omega} = \sqrt{(\mathcal{B}u)^2 - (\Gamma_{zz}-\Gamma_{yy})^2/2}, \quad \bar{\Gamma} = (\Gamma_{zz}+\Gamma_{yy})/2, \tag{9}$$

and the components of the pseudospin relaxation rate tensor are given by (cf. Ref. [79])

$$\Gamma_{zz} = \frac{\left(\Omega_K^{\rm LT}\right)^2\tau}{2}\left(1+\frac{1}{1+(\mathcal{B}u)^2\tau^2}\right), \tag{10a}$$

$$\Gamma_{yy} = \frac{\left(\Omega_K^{\rm LT}\right)^2\tau}{2} + \frac{(\mathcal{C}uK)^2\tau}{2[1+(\mathcal{B}u)^2\tau^2]}, \tag{10b}$$

$$\Gamma_{xx} = \frac{\left(\Omega_K^{\rm LT}\right)^2\tau + (\mathcal{C}uK)^2\tau}{2[1+(\mathcal{B}u)^2\tau^2]}. \tag{10c}$$

In this regime, generally, the pronounced spin beats with the frequency $\mathcal{B}u$ are observed and their damping is described by the $\bar{\Gamma} \ll \Omega, \tau^{-1}$ in Eq. (9), similarly to the Dyakonov-Perel spin relaxation in systems with Rashba and Dresselhaus spin-orbit splitting [79–83].

Figure 3(b) shows an intermediate regime where $\Omega_K^{\rm LT}\tau = 1$. For $\Omega_K^{\rm LT}\tau \sim 1$, one can use the following approximate formula to describe the spin beats:

$$\frac{s_{z,K}(t)}{s_{z,K}(0)} = \cos(\Omega_c t)e^{-\gamma t}, \tag{11}$$

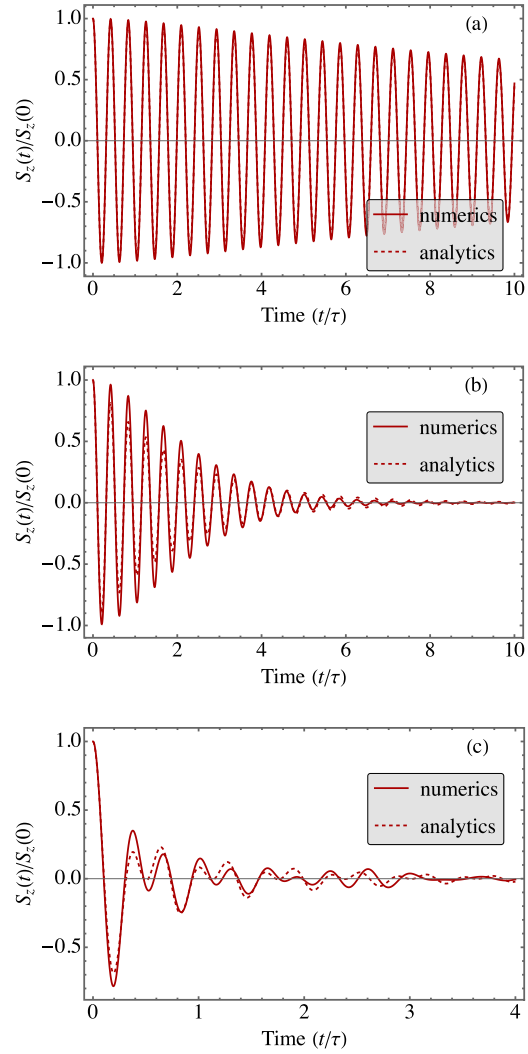

FIG. 3. Temporal dynamics of z component of exciton pseudospin after pulsed circularly polarized excitation calculated by solving kinetic Eq. (4) at $\mathcal{B}u\tau = 15$ (solid lines). (a) $\Omega_K^{\rm LT}\tau = 0.3$, (b) $\Omega_K^{\rm LT}\tau = 1$, and (c) $\Omega_K^{\rm LT}\tau = 5$ (see Fig. 1). Solid curves present numerical results, dotted curves present analytical expressions: Eq. (8) [panel (a)], Eq. (11) [panel (b)], and Eq. (12) [panel (c)].

which captures the main features of the pseudospin dynamics. The spin beats occur at the combination frequency $\Omega_c = \sqrt{(\mathcal{B}u)^2 + (\Omega_K^{\rm LT})^2}$ and decay with the rate $\gamma \approx 1/(2\tau)$.

Finally, in Fig. 3(c) the polarization dynamics in the regime where $\Omega_K^{\rm LT}\tau = 5$ is presented. Here the pronounced beating of exciton pseudospin is seen with two distinct frequencies. A compact expression that describes the polarization dynamics can be derived in the limit where $\tau^{-1} \ll \Omega_K^{\rm LT} \ll \mathcal{B}u$:

$$\frac{s_{z,K}(t)}{s_{z,K}(0)} = \cos(\mathcal{B}ut)\mathrm{J}_0\left(\Omega_K^{\rm LT}t\right)e^{-\gamma t}, \tag{12}$$

with $\mathrm{J}_0(x)$ being the Bessel function. Equation (12) in the limit of $\tau \to \infty$ can be readily obtained averaging the temporal dynamics of the exciton spin-z with a given wave vector $\boldsymbol{K}$: $s_{z,\boldsymbol{K}}(t) \propto \cos(\Omega_{\boldsymbol{K}}t)$ over the directions of $\boldsymbol{K}$. The damping rate $\gamma \approx 1/(2\tau)$ in Eqs. (11) and (12) can be qualitatively understood taking into account the approximately equal relative

weights of the zeroth angular harmonic, which is not affected by the collision integral (6), and other harmonics, which relax with the rate τ^{-1}.

C. Brief discussion

We have studied above the interplay of exciton LT splitting and strain-induced splitting in coherent spin dynamics for monoenergetic quasiparticles with the same $K = |\boldsymbol{K}|$. Such a simple regime can be realized in the absence of inelastic processes, which are indeed weak if the dominant scattering processes are related to the exciton interaction with the long-wavelength phonons and static disorder [69,84].

Let us now briefly address the role of energy relaxation processes. The spread of exciton energies in the course of the energy relaxation leads to a spread of the LT splittings $\Omega_K^{\rm LT}$ and suppresses its contribution to the polarization beats. Thus, in real systems the observation of the beatings described by Eq. (12) can be hampered by the redistribution of excitons over a range of energies.

On the other hand, the strain-induced splitting is wave-vector-independent. Hence, the spin beats caused by the strain are almost insensitive to the energy relaxation processes as long as the dependence of $\mathcal{B}$ on the exciton energy can be disregarded. The damping of these beats can be, however, affected by the energy relaxation processes to the same extent as the energy relaxation processes affect spin relaxation in conventional semiconductors. For instance, in the regime $\tau^{-1} \ll \Omega_K^{\rm LT} \ll \mathcal{B}u$, Eq. (12), a fast initial energy relaxation (or thermalization) of excitons can be accounted for by averaging $\mathrm{J}_0(\Omega_K^{\rm LT} t)$ over an appropriate energy distribution of excitons. For fully thermalized excitons to the temperature T, we obtain

$$\left\langle \mathrm{J}_0\left(\Omega_K^{\rm LT} t\right)\right\rangle = \exp\left(-\frac{(\Omega_{K_T}^{\rm LT})^2 t^2}{4}\right), \quad K_T = \sqrt{\frac{2Mk_BT}{\hbar^2}}.$$

Here M is the exciton translational mass (typically $M \sim m_0$ is the free-electron mass in TMDC MLs) and K_T is the thermal wave vector. Correspondingly, $\Omega_{K_T}^{\rm LT}$ gives the rate of the polarization decay in this regime. By contrast, in the regime $\Omega_{K_T}^{\rm LT}\tau \ll 1$, Eqs. (8) and (9) hold but the rates Γ_{ij} in Eq. (10) should be appropriately averaged over the energy distribution of the excitons in the regime of fast energy relaxation as compared to the pseudospin relaxation, $\tau_\epsilon \bar{\Gamma} \ll 1$, or Eq. (8) should be averaged over the thermal distribution in the opposite limit $\tau_\epsilon \bar{\Gamma} \gg 1$, with τ_ϵ being the energy relaxation time.

We also note that in real structures the components of the strain tensor u_{ij} can be random functions of coordinates due to inevitable inhomogeneities of the systems. Such spatial fluctuations of strain produce spatial fluctuations of the exciton fine-structure splitting and act similarly to the random Rashba fields and spin-orbit coupling disorder in quantum wells [85,86]. The strain fluctuations produce a lower bound to the exciton spin or valley relaxation rate,

$$\gamma_{\rm min} \sim \begin{cases} \mathcal{B}^2\langle \delta u^2\rangle \tau_c, & \tau_c \ll \tau, \quad \mathcal{B}^2\langle \delta u^2\rangle \tau_c^2 \ll 1, \\ \mathcal{B}\sqrt{\langle \delta u^2\rangle}, & \mathcal{B}^2\langle \delta u^2\rangle \gg \tau^{-2}, \tau_c^{-2}. \end{cases} \tag{13}$$

Here $\langle \delta u^2\rangle$ is the mean square of the strain fluctuation and $\tau_c = l_c/(\hbar K/M)$ is the correlation time, with l_c being the correlation length of the strain fluctuations, and we assumed that $\langle \delta u\rangle = 0$. A spatial dependence of strain and, hence, of the exciton fine-structure splitting can be particularly important in moiré structures formed in TMDC bilayers [87].

IV. CONCLUSION AND OUTLOOK

In this work, we have focused on the temporal dynamics of exciton spin polarization. Under the steady-state excitation conditions, a pronounced effect of the strain on the exciton optical orientation is expected. Similarly to Ref. [88], the exciton optical orientation can be a nonmonotonous function of the strain due to a competition of the LT and strain-induced splittings of excitonic states. An interplay of the LT and strain-induced contributions can also be observed in the exciton pseudospin fluctuations, cf. [89,90], and it affects valley polarization bistability and its stochastic switching [64].

The exciton spin beats studied here can be observed in time-resolved experiments where the superposition of the strain-split states is created by a short circularly polarized light pulse resonant or quasiresonant with the excitonic transition. The dynamics can be monitored by the time-resolved circular and linear polarization degree of exciton emission or via the Kerr or Faraday rotation of the polarization plane of the additional linearly polarized probe pulse; see Refs. [23,50,51] for details.

In conclusion, we have theoretically studied exciton spin dynamics in two-dimensional semiconductors based on transition-metal dichalcogenides focusing on the strain effects. We have demonstrated an interplay of the exciton radiative doublet longitudinal-transverse and strain-induced splittings in the spin beats of excitons. The regimes where the exciton circular polarization beats are controlled by the strain have been identified. In the case in which both longitudinal-transverse and strain-induced splittings of the exciton radiative doublet are sufficiently large, two frequencies in the exciton spin beats appear. The damping of the exciton spin precession has also been analyzed. Compact analytical expressions that describe numerical results are presented. The role of energy relaxation and strain fluctuations has been discussed.

ACKNOWLEDGMENT

This work has been supported by the RSF Project No. 19-12-00051.

[1] E. I. Rashba, Effect of resonance excitation transfer in the theory of a large radius exciton, JETP **9**, 1213 (1959).

[2] G. Dresselhaus, Effective mass approximation for excitons, J. Phys. Chem. Solids **1**, 14 (1956).

[3] S. I. Pekar, The theory of electromagnetic waves in a crystal in which excitons are produced, JETP **6**, 785 (1958).

[4] J. J. Hopfield, Theory of the contribution of excitons to the complex dielectric constant of crystals, Phys. Rev. **112**, 1555 (1958).

[5] S. I. Pekar, The energy of excitons for very small quasi-momenta, JETP **8**, 360 (1959).
[6] G. E. Pikus and G. L. Bir, Exchange interaction in excitons in semiconductors, JETP **33**, 108 (1971).
[7] M. M. Denisov and V. P. Makarov, Longitudinal and transverse excitons in semiconductors, Phys. Status Solidi B **56**, 9 (1973).
[8] V. A. Kiselev and A. G. Zhilich, Coulomb excitons in semiconductors and exchange interaction screening, Sov. Phys. Solid State **13**, 2008 (1972).
[9] M. Z. Maialle, E. A. de Andrada e Silva, and L. J. Sham, Exciton spin dynamics in quantum wells, Phys. Rev. B **47**, 15776 (1993).
[10] H. Nickolaus, H.-J. Wünsche, and F. Henneberger, Exciton Spin Relaxation in Semiconductor Quantum Wells: The Role of Disorder, Phys. Rev. Lett. **81**, 2586 (1998).
[11] S. V. Goupalov, E. L. Ivchenko, and A. V. Kavokin, Fine structure of localized exciton levels in quantum wells, J. Exp. Theor. Phys. **86**, 388 (1998).
[12] M. Z. Maialle, Spin dynamics of localized excitons in semiconductor quantum wells in an applied magnetic field, Phys. Rev. B **61**, 10877 (2000).
[13] S. V. Goupalov, P. Lavallard, G. Lamouche, and D. S. Citrin, Electrodynamical treatment of the electron-hole long-range exchange interaction in semiconductor nanocrystals, Phys. Solid State **45**, 768 (2003).
[14] E. L. Ivchenko, *Optical Spectroscopy of Semiconductor Nanostructures* (Alpha Science, Harrow, UK, 2005).
[15] S. V. Goupalov, Anisotropy-induced exchange splitting of exciton radiative doublet in CdSe nanocrystals, Phys. Rev. B **74**, 113305 (2006).
[16] M. A. Becker, R. Vaxenburg, G. Nedelcu, P. C. Sercel, A. Shabaev, M. J. Mehl, J. G. Michopoulos, S. G. Lambrakos, N. Bernstein, J. L. Lyons, T. Stöferle, R. F. Mahrt, M. V. Kovalenko, D. J. Norris, G. Rainò, and A. L. Efros, Bright triplet excitons in caesium lead halide perovskites, Nature (London) **553**, 189 (2018).
[17] R. Ben Aich, I. Saïdi, S. Ben Radhia, K. Boujdaria, T. Barisien, L. Legrand, F. Bernardot, M. Chamarro, and C. Testelin, Bright-Exciton Splittings in Inorganic Cesium Lead Halide Perovskite Nanocrystals, Phys. Rev. Appl. **11**, 034042 (2019).
[18] I. D. Avdeev, M. O. Nestoklon, and S. V. Goupalov, Exciton fine structure in lead chalcogenide quantum dots: Valley mixing and crucial role of intervalley electron–hole exchange, Nano Lett. **20**, 8897 (2020).
[19] S. V. Goupalov, E. L. Ivchenko, and M. O. Nestoklon, Optical transitions, exciton radiative decay, and valley coherence in lead chalcogenide quantum dots, Phys. Rev. B **106**, 125301 (2022).
[20] M. M. Glazov, T. Amand, X. Marie, D. Lagarde, L. Bouet, and B. Urbaszek, Exciton fine structure and spin decoherence in monolayers of transition metal dichalcogenides, Phys. Rev. B **89**, 201302(R) (2014).
[21] H. Yu, G.-B. Liu, P. Gong, X. Xu, and W. Yao, Dirac cones and Dirac saddle points of bright excitons in monolayer transition metal dichalcogenides, Nat. Commun. **5**, 3876 (2014).
[22] T. Yu and M. W. Wu, Valley depolarization due to intervalley and intravalley electron-hole exchange interactions in monolayer MoS_2, Phys. Rev. B **89**, 205303 (2014).
[23] C. R. Zhu, K. Zhang, M. Glazov, B. Urbaszek, T. Amand, Z. W. Ji, B. L. Liu, and X. Marie, Exciton valley dynamics probed by Kerr rotation in WSe_2 monolayers, Phys. Rev. B **90**, 161302(R) (2014).
[24] M. M. Glazov, E. L. Ivchenko, G. Wang, T. Amand, X. Marie, B. Urbaszek, and B. L. Liu, Spin and valley dynamics of excitons in transition metal dichalcogenide monolayers, Phys. Status Solidi B **252**, 2349 (2015).
[25] A. I. Prazdnichnykh, M. M. Glazov, L. Ren, C. Robert, B. Urbaszek, and X. Marie, Control of the exciton valley dynamics in atomically thin semiconductors by tailoring the environment, Phys. Rev. B **103**, 085302 (2021).
[26] M. Dyksik, H. Duim, D. K. Maude, M. Baranowski, M. A. Loi, and P. Plochocka, Brightening of dark excitons in 2D perovskites, Sci. Adv. **7**, eabk0904 (2021).
[27] D. Xiao, G.-B. Liu, W. Feng, X. Xu, and W. Yao, Coupled Spin and Valley Physics in Monolayers of MoS_2 and Other Group-VI Dichalcogenides, Phys. Rev. Lett. **108**, 196802 (2012).
[28] A. K. Geim and I. V. Grigorieva, Van der Waals heterostructures, Nature (London) **499**, 419 (2013).
[29] A. V. Kolobov and J. Tominaga, *Two-Dimensional Transition-Metal Dichalcogenides* (Springer International, Berlin, 2016).
[30] G. Wang, A. Chernikov, M. M. Glazov, T. F. Heinz, X. Marie, T. Amand, and B. Urbaszek, Colloquium: Excitons in atomically thin transition metal dichalcogenides, Rev. Mod. Phys. **90**, 021001 (2018).
[31] H. Rostami, R. Roldán, E. Cappelluti, R. Asgari, and F. Guinea, Theory of strain in single-layer transition metal dichalcogenides, Phys. Rev. B **92**, 195402 (2015).
[32] K. Zollner, P. E. F. Junior, and J. Fabian, Strain-tunable orbital, spin-orbit, and optical properties of monolayer transition-metal dichalcogenides, Phys. Rev. B **100**, 195126 (2019).
[33] A. Castellanos-Gomez, R. Roldán, E. Cappelluti, M. Buscema, F. Guinea, H. S. J. van der Zant, and G. A. Steele, Local strain engineering in atomically thin MoS_2, Nano Lett. **13**, 5361 (2013).
[34] M. Brooks and G. Burkard, Theory of strain-induced confinement in transition metal dichalcogenide monolayers, Phys. Rev. B **97**, 195454 (2018).
[35] A. Smiri, T. Amand, and S. Jaziri, Optical properties of excitons in two-dimensional transition metal dichalcogenide nanobubbles, J. Chem. Phys. **154**, 084110 (2021).
[36] H. Moon, G. Grosso, C. Chakraborty, C. Peng, T. Taniguchi, K. Watanabe, and D. Englund, Dynamic exciton funneling by local strain control in a monolayer semiconductor, Nano Lett. **20**, 6791 (2020).
[37] H. Lee, K. Yeonjeong, C. Jinseong, K. Shailabh, L. Hyoung-Taek, J. Gangseon, C. S. Ho, K. Mingu, K. K. Kang, P. Hyeong-Ryeol, C. Hyuck, and P. Kyoung-Duck, Drift-dominant exciton funneling and trion conversion in 2D semiconductors on the nanogap, Sci. Adv. **8**, eabm5236 (2022).
[38] Y. Bai, L. Zhou, J. Wang, W. Wu, L. J. McGilly, D. Halbertal, C. F. B. Lo, F. Liu, J. Ardelean, P. Rivera, N. R. Finney, X.-C. Yang, D. N. Basov, W. Yao, X. Xu, J. Hone, A. N. Pasupathy, and X. Y. Zhu, Excitons in strain-induced one-dimensional moiré potentials at transition metal dichalcogenide heterojunctions, Nat. Mater. **19**, 1068 (2020).
[39] R. Rosati, R. Schmidt, S. Brem, R. Perea-Causín, I. Niehues, J. Kern, J. A. Preuß, R. Schneider, S. Michaelis de Vasconcellos, R. Bratschitsch, and E. Malic, Dark exciton anti-funneling in atomically thin semiconductors, Nat. Commun. **12**, 7221 (2021).

[40] V. Shahnazaryan and H. Rostami, Nonlinear exciton drift in piezoelectric two-dimensional materials, Phys. Rev. B **104**, 085405 (2021).

[41] F. Dirnberger, Z. Jonas, P. Faria Junior, R. Bushati, T. Taniguchi, K. Watanabe, J. Fabian, D. Bougeard, A. Chernikov, and V. Menon, Quasi-1D exciton channels in strain-engineered 2D materials, Sci. Adv. **7**, eabj3066 (2021).

[42] Z. Peng, X. Chen, Y. Fan, D. J. Srolovitz, and D. Lei, Strain engineering of 2D semiconductors and graphene: From strain fields to band-structure tuning and photonic applications, Light: Sci. Appl. **9**, 190 (2020).

[43] A. Mitioglu, S. Anghel, M. V. Ballottin, K. Sushkevich, L. Kulyuk, and P. C. M. Christianen, Anomalous rotation of the linearly polarized emission of bright excitons in strained WSe_2 monolayers under high magnetic fields, Phys. Rev. B **99**, 155414 (2019).

[44] J. Jasinski, A. Balgarkashi, V. Piazza, D. Dede, A. Surrente, M. Baranowskki, D. K. Maude, M. Banerjee, R. Frisenda, A. Castellanos-Gomez, A. Fontcuberta i Morral, and P. Plochocka, Strain induced lifting of the charged exciton degeneracy in monolayer MoS_2 on a GaAs nanomembrane, 2D Mater. **9**, 045006 (2022).

[45] M. M. Glazov, F. Dirnberger, V. M. Menon, T. Taniguchi, K. Watanabe, D. Bougeard, J. D. Ziegler, and A. Chernikov, Exciton fine structure splitting and linearly polarized emission in strained transition-metal dichalcogenide monolayers, Phys. Rev. B **106**, 125303 (2022).

[46] E. I. Rashba and V. I. Sheka, Symmetry of energy bands in crystals of wurtzite type. II. Symmetry of bands with spin-orbit interaction included, Fiz. Tverd. Tela: Collected Papers **2**, 162 (1959).

[47] E. I. Rashba, Properties of semiconductors with an extremum loop. I. Cyclotron and combinational resonance in a magnetic field perpendicular to the plane of the loop, Sov. Phys. Solid State **2**, 1109 (1960).

[48] Y. Bychkov and E. Rashba, Oscillatory effects and the magnetic susceptibility of carriers in inversion layers, J. Phys. C **17**, 6039 (1984).

[49] E. I. Rashba and A. L. Efros, Orbital Mechanisms of Electron-Spin Manipulation by an Electric Field, Phys. Rev. Lett. **91**, 126405 (2003).

[50] D. R. Yakovlev and M. Bayer, Coherent spin dynamics of carriers, in *Spin Physics in Semiconductors*, 2nd ed., Springer Series in Solid-State Sciences 157, edited by M. I. Dyakonov (Springer International, Berlin, 2017), p. 155.

[51] X. Marie and T. Amand, Exciton spin dynamics in semiconductor quantum wells, in *Spin Physics in Semiconductors*, 2nd ed., Springer Series in Solid-State Sciences 157, edited by M. I. Dyakonov (Springer International, Berlin, 2017), p. 69.

[52] G. Kioseoglou, A. T. Hanbicki, M. Currie, A. L. Friedman, D. Gunlycke, and B. T. Jonker, Valley polarization and intervalley scattering in monolayer MoS_2, Appl. Phys. Lett. **101**, 221907 (2012).

[53] H. Zeng, J. Dai, W. Yao, D. Xiao, and X. Cui, Valley polarization in MoS_2 monolayers by optical pumping, Nat. Nanotechnol. **7**, 490 (2012).

[54] G. Sallen, L. Bouet, X. Marie, G. Wang, C. R. Zhu, W. P. Han, Y. Lu, P. H. Tan, T. Amand, B. L. Liu, and B. Urbaszek, Robust optical emission polarization in MoS_2 monolayers through selective valley excitation, Phys. Rev. B **86**, 081301(R) (2012).

[55] K. F. Mak, K. He, J. Shan, and T. F. Heinz, Control of valley polarization in monolayer MoS_2 by optical helicity, Nat. Nanotechnol. **7**, 494 (2012).

[56] A. M. Jones, H. Yu, N. J. Ghimire, S. Wu, G. Aivazian, J. S. Ross, B. Zhao, J. Yan, D. G. Mandrus, D. Xiao, W. Yao, and X. Xu, Optical generation of excitonic valley coherence in monolayer WSe_2, Nat. Nanotechnol. **8**, 634 (2013).

[57] G. Wang, X. Marie, B. L. Liu, T. Amand, C. Robert, F. Cadiz, P. Renucci, and B. Urbaszek, Control of Exciton Valley Coherence in Transition Metal Dichalcogenide Monolayers, Phys. Rev. Lett. **117**, 187401 (2016).

[58] A. Krasnok and A. Alù, Valley-selective response of nanostructures coupled to 2D transition-metal dichalcogenides, Appl. Sci. **8**, 1157 (2018).

[59] M. M. Glazov and E. L. Ivchenko, Valley orientation of electrons and excitons in atomically thin transition metal dichalcogenide monolayers (brief review), JETP Lett. **113**, 7 (2021).

[60] G. L. Bir and G. E. Pikus, *Symmetry and Strain-induced Effects in Semiconductors* (Wiley/Halsted, New York, Toronto, 1974).

[61] M. Yang, C. Robert, Z. Lu, D. Van Tuan, D. Smirnov, X. Marie, and H. Dery, Exciton valley depolarization in monolayer transition-metal dichalcogenides, Phys. Rev. B **101**, 115307 (2020).

[62] C. Robert, B. Han, P. Kapuscinski, A. Delhomme, C. Faugeras, T. Amand, M. R. Molas, M. Bartos, K. Watanabe, T. Taniguchi, B. Urbaszek, M. Potemski, and X. Marie, Measurement of the spin-forbidden dark excitons in MoS_2 and $MoSe_2$ monolayers, Nat. Commun. **11**, 4037 (2020).

[63] A. Kavokin, G. Malpuech, and M. Glazov, Optical Spin Hall Effect, Phys. Rev. Lett. **95**, 136601 (2005).

[64] M. A. Semina, M. M. Glazov, C. Robert, L. Lombez, T. Amand, and X. Marie, Valley polarization fluctuations, bistability, and switching in two-dimensional semiconductors, Phys. Rev. B **106**, 035302 (2022).

[65] A. Kormanyos, G. Burkard, M. Gmitra, J. Fabian, V. Zólyomi, N. D. Drummond, and V. Fal'ko, $\boldsymbol{k}\cdot\boldsymbol{p}$ theory for two-dimensional transition metal dichalcogenide semiconductors, 2D Mater. **2**, 022001 (2015).

[66] D. V. Rybkovskiy, I. C. Gerber, and M. V. Durnev, Atomically inspired $\boldsymbol{k}\cdot\boldsymbol{p}$ approach and valley Zeeman effect in transition metal dichalcogenide monolayers, Phys. Rev. B **95**, 155406 (2017).

[67] C. Grimaldi, Electron spin dynamics in impure quantum wells for arbitrary spin-orbit coupling, Phys. Rev. B **72**, 075307 (2005).

[68] N. S. Averkiev and M. M. Glazov, Specific features of optical orientation and relaxation of electron spins in quantum wells with a large spin splitting, Semiconductors **42**, 958 (2008).

[69] M. M. Glazov, Quantum Interference Effect on Exciton Transport in Monolayer Semiconductors, Phys. Rev. Lett. **124**, 166802 (2020).

[70] K. Wagner, J. Zipfel, R. Rosati, E. Wietek, J. D. Ziegler, S. Brem, R. Perea-Causín, T. Taniguchi, K. Watanabe, M. M. Glazov, E. Malic, and A. Chernikov, Nonclassical Exciton Diffusion in Monolayer WSe_2, Phys. Rev. Lett. **127**, 076801 (2021).

[71] S. Shree, M. Semina, C. Robert, B. Han, T. Amand, A. Balocchi, M. Manca, E. Courtade, X. Marie, T. Taniguchi, K. Watanabe, M. M. Glazov, and B. Urbaszek, Observation of exciton-phonon coupling in $MoSe_2$ monolayers, Phys. Rev. B **98**, 035302 (2018).

[72] M. M. Glazov, Effect of structure anisotropy on low temperature spin dynamics in quantum wells, Solid State Commun. **142**, 531 (2007).

[73] R. I. Dzhioev, H. M. Gibbs, E. L. Ivchenko, G. Khitrova, V. L. Korenev, M. N. Tkachuk, and B. P. Zakharchenya, Determination of interface preference by observation of linear-to-circular polarization conversion under optical orientation of excitons in type-II GaAs/AlAs superlattices, Phys. Rev. B **56**, 13405 (1997).

[74] G. V. Astakhov, T. Kiessling, A. V. Platonov, T. Slobodskyy, S. Mahapatra, W. Ossau, G. Schmidt, K. Brunner, and L. W. Molenkamp, Circular-to-Linear and Linear-to-Circular Conversion of Optical Polarization by Semiconductor Quantum Dots, Phys. Rev. Lett. **96**, 027402 (2006).

[75] K. Kowalik, O. Krebs, A. Lemaître, J. A. Gaj, and P. Voisin, Optical alignment and polarization conversion of the neutral-exciton spin in individual InAs/GaAs quantum dots, Phys. Rev. B **77**, 161305(R) (2008).

[76] J. Michl, C. C. Palekar, S. A. Tarasenko, F. Lohof, C. Gies, M. von Helversen, R. Sailus, S. Tongay, T. Taniguchi, K. Watanabe, T. Heindel, B. Rosa, M. Rödel, T. Shubina, S. Höfling, S. Reitzenstein, C. Anton-Solanas, and C. Schneider, Intrinsic circularly polarized exciton emission in a twisted van der Waals heterostructure, Phys. Rev. B **105**, L241406 (2022).

[77] V. Kalevich, B. Zakharchenya, K. Kavokin, A. Petrov, P. Le Jeune, X. Marie, D. Robart, T. Amand, J. Barrau, and M. Brousseau, Determination of the sign of the conduction-electron *g* factor in semiconductor quantum wells by means of the Hanle effect and spin-quantum-beat techniques, Phys. Solid State **39**, 681 (1997).

[78] M. M. Glazov and E. L. Ivchenko, Resonant spin amplification in nanostructures with anisotropic spin relaxation and spread of the electronic *g*-factor, Semiconductors **42**, 951 (2008).

[79] M. M. Glazov, Magnetic field effects on spin relaxation in heterostructures, Phys. Rev. B **70**, 195314 (2004).

[80] M. Dyakonov and V. Perel', Spin relaxation of conduction electrons in noncentrosymmetric semiconductors, Sov. Phys. Solid State **13**, 3023 (1972).

[81] M. Dyakonov and V. Kachorovskii, Spin relaxation of two-dimensional electrons in noncentrosymmetric semiconductors, Sov. Phys. Semicond. **20**, 110 (1986).

[82] E. L. Ivchenko, Spin relaxation of free carriers in a noncentrosymmetric semiconductor in a longitudinal magnetic field, Sov. Phys. Solid State **15**, 1048 (1973).

[83] E. L. Ivchenko, P. S. Kop'ev, V. P. Kochereshko, I. N. Ural'tsev, and D. R. Yakovlev, Optical orientation of electrons and holes in semiconductor superlattices, JETP Lett. **47**, 486 (1988).

[84] M. M. Glazov, Z. A. Iakovlev, and S. Refaely-Abramson, Phonon-induced exciton weak localization in two-dimensional semiconductors, Appl. Phys. Lett. **121**, 192106 (2022).

[85] E. Y. Sherman, Random spin-orbit coupling and spin relaxation in symmetric quantum wells, Appl. Phys. Lett. **82**, 209 (2003).

[86] M. Glazov, E. Sherman, and V. Dugaev, Two-dimensional electron gas with spin-orbit coupling disorder, J. Phys. E **42**, 2157 (2010).

[87] A. Tartakovskii, Excitons in 2D heterostructures, Nat. Rev. Phys. **2**, 8 (2020).

[88] A. V. Poshakinskiy and S. A. Tarasenko, Spin-orbit Hanle effect in high-mobility quantum wells, Phys. Rev. B **84**, 073301 (2011).

[89] D. S. Smirnov and M. M. Glazov, Exciton spin noise in quantum wells, Phys. Rev. B **90**, 085303 (2014).

[90] M. M. Glazov, M. A. Semina, E. Y. Sherman, and A. V. Kavokin, Spin noise of exciton polaritons in microcavities, Phys. Rev. B **88**, 041309(R) (2013).